

A NOVEL TRI-MODE BANDWIDTH TUNABLE FILTER WITH HARMONIC SUPPRESSION

D.-H. Jia, Q.-Y. Feng^{*}, X.-G. Huang, and Q.-Y. Xiang

School of Information Science and Technology, Southwest Jiaotong University, Chengdu, Sichuan 610031, China

Abstract—In this paper, a novel bandwidth reconfigurable bandpass filter is proposed. Based on a varactor loaded tri-mode resonator consisted of one constant odd mode and two independent varactor-tuned even modes, each passband edge of the proposed filter can be freely adjusted. By varying the reverse bias voltage applied to the varactor diode that is connected to the resonator, the bandwidth can be controlled conveniently. The resonant frequencies and Transmission Zeros (TZs) are derived and verified by both theoretical analysis and simulation. Stepped Impedance Resonator (SIR) is introduced to optimize the harmonic suppression. Finally, the measurement of the fabricated filter shows a fractional bandwidth tuning range of 11.4–32.0% with a center frequency of 1.75 GHz, a quite low insertion loss of 0.4–1.1 dB, and wideband harmonic suppression up to 6 GHz. The measurement and simulated results show good agreement.

1. INTRODUCTION

Due to their potential to significantly reduce the overall size and complexity of modern multiband communication systems [1–3], RF tunable filters are becoming an active research topic. To the best of our knowledge, there are three types of tunable filters: center frequency tunable filters with predefined bandwidth [4–8], bandwidth tunable filter [9–11], and both center frequency and bandwidth tunable filters [12–15].

Among the tunable filter designs above, the bandwidth tunable character is less discussed in comparison with reconfigurable center frequency. In [9–11], bandwidth tunable filters were proposed. In [9], a ring resonator bandpass filter with switchable bandwidth was

Received 25 September 2012, Accepted 7 November 2012, Scheduled 9 November 2012

* Corresponding author: Quanyuan Feng (fengquanyuan@163.com).

presented. PIN diodes and Stepped-Impedance stubs were adopted to bandwidth tuning. Varactor tuned quadruple-mode bandpass filter with separate lower/upper bandwidth was reported in [10]. In [12], a dual-mode triangular patch bandpass filter was proposed. Two slots assembled with varactor diodes were used to vary the frequency of each degenerate fundamental mode independently. With this method, both center frequency and bandwidth could be controlled independently. However, the issue of spurious passbands was not addressed in those works.

In this paper, a novel tri-mode bandwidth tunable bandpass filter is built, which contains two even-modes, one odd mode in the desired passband and two Transmission Zeros (TZs) near the upper and lower stopbands. Each of the TZs can be separately adjusted to relocate the corresponding passband edge. Even- and odd-mode equivalent circuits of the filter are proposed to calculate the resonant frequencies and transmission zeros. After that, Stepped Impedance Resonator (SIR) is adopted to enhance harmonic suppression performance. Finally, a bandwidth tunable bandpass filter based on tri-mode sub-loaded resonator is designed, fabricated, and measured.

2. FILTER DESIGN

Figure 1(a) shows the layout of the proposed bandwidth tunable BPF based on a tri-mode resonator. The resonator consists of one half wavelength resonator, two varactor-loaded stubs shunted at the center plane. Two capacitors C_{in} were connected between the feed lines

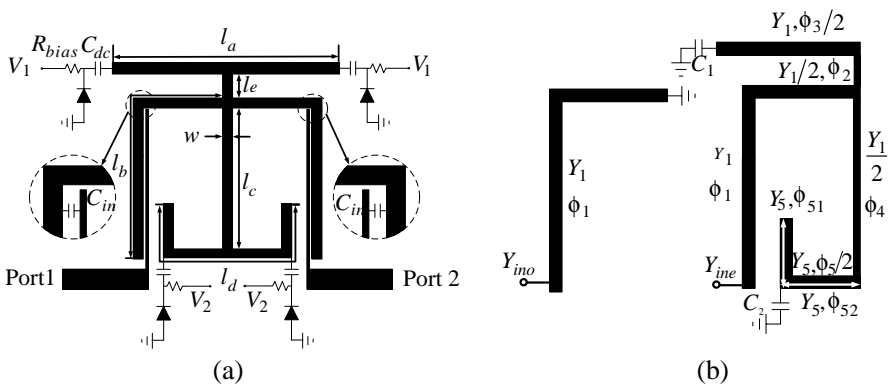


Figure 1. (a) Layout of the bandwidth tunable bandpass filter without harmonic suppression. (b) Odd and even mode equivalent circuit.

and the tri-mode resonator, as shown in Figure 1(a), to achieve the desired coupling, instead of placing the feed line closer to the resonator, which would lead to unacceptable technological constrains. Since the structure is symmetrical to the centra plane, the even-odd-mode analysis method can be adopted, as depicted in Figure 1(b). C_1 and C_2 are the variable loading capacitance of the stubs. All the width of the resonators is chosen as w so that all the characteristic admittances is Y_1 , and l_a, l_b, l_c, l_d, l_e refer to the length parameter of the resonator in Figure 1(a). The resonant conditions can be achieved and expressed as

$$Y_{ino} = -jY_1 \cot \phi_1 \tag{1}$$

$$Y_{ine} = Y_1 \frac{(Y_{L11} + Y_{L12}) + jY_1 \tan \phi_1}{Y_1 + j(Y_{L11} + Y_{L12}) \tan \phi_1} \tag{2}$$

where

$$Y_{L11} = \frac{Y_1}{2} \cdot \frac{Y_{L1} + (jY_1 \tan \phi_2)/2}{Y_1/2 + jY_{L1} \tan \phi_2},$$

$$Y_{L12} = \frac{Y_1}{2} \cdot \frac{Y_1 \frac{Y_{L2} + jY_1 \tan \phi_{52}}{Y_1 + jY_{L2} \tan \phi_{52}} + (jY_1 \tan \phi_4)/2}{Y_1/2 + jY_1 \frac{Y_{L2} + jY_1 \tan \phi_{52}}{Y_1 + jY_{L2} \tan \phi_{52}} \tan \phi_4},$$

$$Y_{L1} = jY_1 \frac{\omega C_1 + Y_3 \tan(\phi_3/2)}{Y_1 - \omega C_1 \tan(\phi_3/2)}, \quad Y_{L2} = j(\omega C_2 + Y_1 \tan \phi_{51}).$$

The transmission zero frequencies are obtained when $Y_{21} = Y_{12} = 0$. The filter TZs can be calculated by

$$Y_{12} = \frac{Y_1^2}{Y_{L11} \cdot \sin^2 \phi + Y_{L12} \cdot \sin^2 \phi - jY_1 \sin 2\phi} \tag{3}$$

while

$$Y_{L11} \rightarrow \infty, \quad Y_{L12} \rightarrow \infty$$

It can be observed from Formulas (1) and (2) that the stepped-impedance varactor-loaded stub at the center plane merely controls resonant frequencies of even excitation. In order to achieve the detailed scheme of the resonant modes and TZs, an instructive method is adopted [13], as shown in Figure 2. In this method the resonator is driven through a weak coupling. In Figure 2(a), the common characteristic can be obtained that the even-mode resonant frequencies decreases while increasing the length l_a or l_d . The conclusion can be made here that the lower resonant frequency is the first even-mode frequency which is controlled by inner stub. The middle resonant frequency is the first odd-mode frequency which is controlled by the l_b shown by Formula (1). Then the third resonant frequency is the

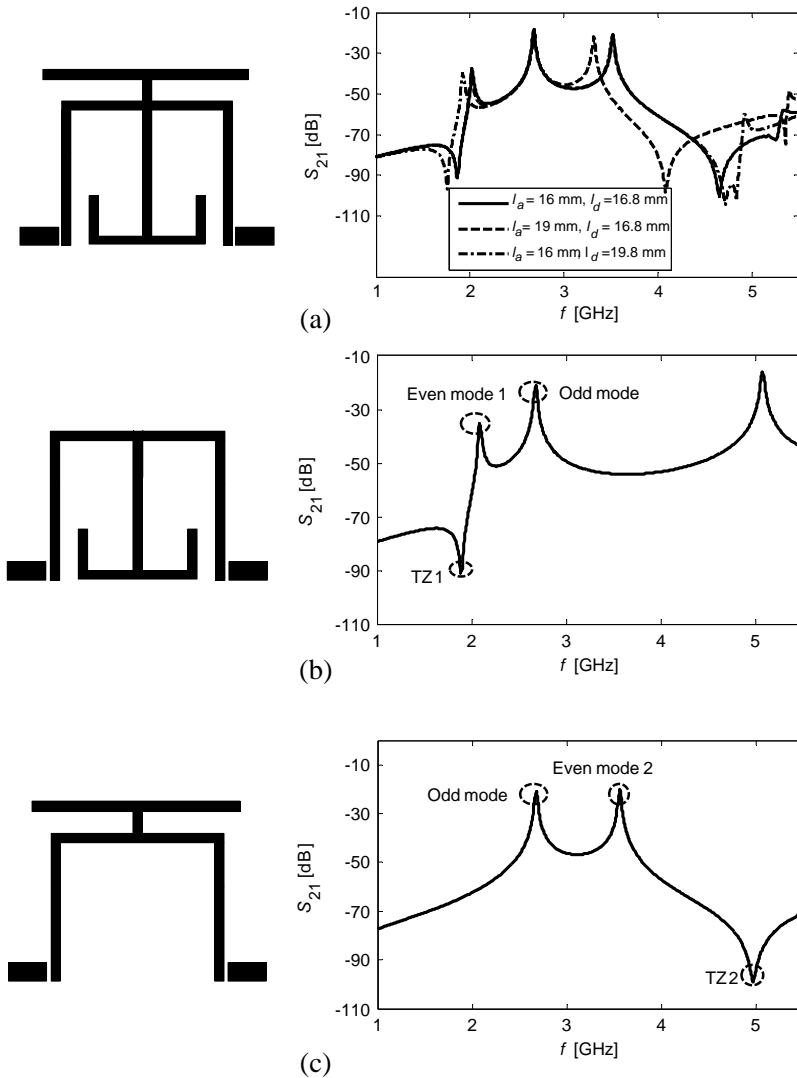


Figure 2. Resonant-mode frequencies and TZs analysis. (a) Tri-mode resonator for different values of l_a or l_b . (b) Dual-mode resonator with inner stub. (c) Dual-mode resonator with outer stub.

second even-mode frequency, which is controlled by the outer stub. By observing the simulated results presented in Figures 2(b) and (c), the TZ1 is excited by the even-mode1 and the odd-mode part, meanwhile, the TZ2 is generated by the even-mode2 and the odd-mode part.

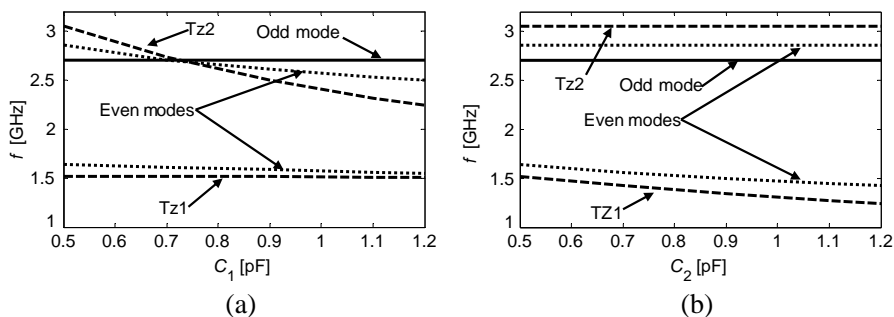


Figure 3. Resonant-mode frequencies and TZs. (a) $C_2 = 0.5$ pF, varying C_1 . (b) $C_1 = 0.5$ pF, varying C_2 .

Finally, we can get the unique property of the tri-mode resonator that the even mode resonant frequencies and TZs can be controlled by adjusting the flexible parameters of the stubs, whereas the odd mode resonant frequency can hardly be changed.

The resonant frequencies and TZs can be calculated by the Formulas (1)–(3), as shown in Figure 3. It is obvious that there are one odd mode, two even modes and two transmission zeros in the frequency range 1–3.5 GHz. In Figure 3(a), the higher even mode and TZ2 move toward the lower frequency when $C_2 = 0.5$ pF and C_1 varies from 0.5 pF to 1.2 pF. Lower even mode and TZ1 show slim variation and the odd mode remains constant. When $C_1 = 0.5$ pF and C_2 varies from 0.5 pF to 1.2 pF, as presented in Figure 3(b), the lower even mode and TZ1 move toward the lower frequency, while the odd mode, higher even mode and TZ2 remaining unchanged. Through the analysis above, the higher even mode and TZ2 can be controlled by varying C_1 . Simultaneous, the lower even mode and TZ1 can be adjusted by varying C_2 .

This unique property can be used to design bandwidth tunable filter. Inspired by it, a bandwidth tunable BPF is designed, simulated for $\epsilon_r = 2.65$ and $h = 0.5$ mm. The simulation model of the varactor C_1 and C_2 is implemented with SKYWORKS SMV1405 spice model. The single varactor capacitance is 0.63 pF and 2.67 pF at 30 V and 0 V reverse bias, respectively. The value of C_{in} was optimized to be 1.4 pF for the tunability. The dimensions of the filter is $w = 0.8$ mm, $l_a = 16.0$ mm, $l_b = 19.1$ mm, $l_c = 13.4$ mm, $l_d = 18.4$ mm, $l_e = 1.9$ mm.

Figure 4 illustrates simulated results of the bandwidth tunable BPF. The -3 dB bandwidth ranges from 180 MHz to 680 MHz with a fixed centra frequency, 1.6 GHz.

However, the out band rejection of this filter is poor due to

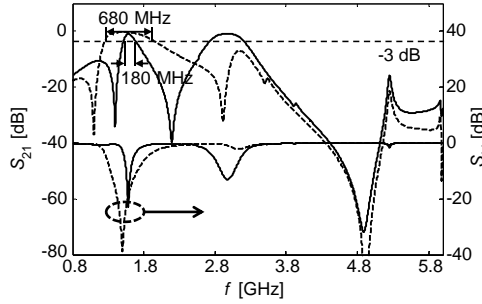


Figure 4. Simulated S -parameters of the bandwidth tunable filter without harmonic suppression.

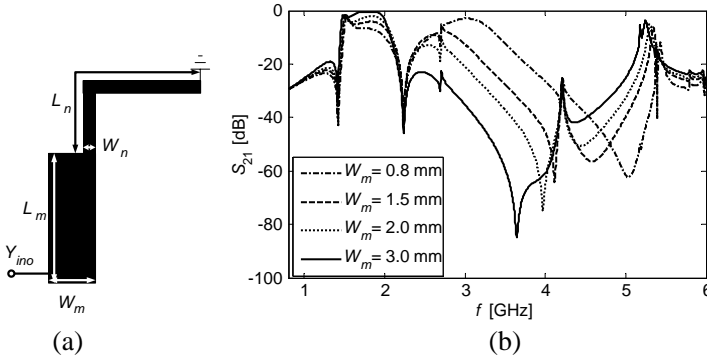


Figure 5. The harmonic suppression analysis of the changed odd mode part. (a) The odd-mode part introduced with SIR. (b) The simulated results while fixed W_n , L_n and L_m , varying W_m .

the existence of second harmonic. In order to suppress the second harmonic, through the analysis of the filter structure, the odd mode part offers the most important influence on the performance of the harmonic suppression. SIR (Stepped Impedance Resonator) is introduced to this filter to suppress the harmonic, as shown in Figure 5(a). Figure 5(b) shows the simulated frequency response of the filter against different W_m/W_n and a constant L_m/L_n . The second harmonic of the filter can be suppressed efficiently by tuning W_m while keeping $W_n = 0.8$ mm, $L_n = 8.2$ mm, $L_m = 11.2$ mm. The suppression effect on harmonic is very obvious while W_m increasing from 2 to 3 mm.

As illustrated in Figure 6, W_m/W_n shows its great influence on the second harmonic suppression by varying the the location of transmission zeros. Finally, as a tradeoff between the tunability

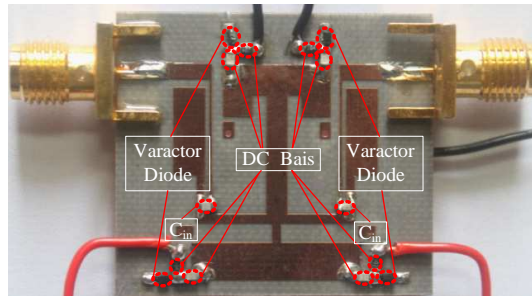


Figure 7. Fabricated bandwidth tunable BPF with harmonic suppression.

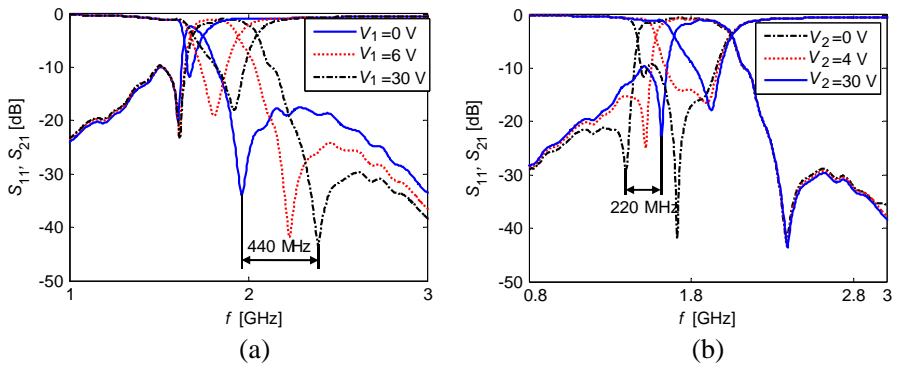


Figure 8. Measured S -parameters for upper and lower bandgap tuning. (a) Fixed $V_2 = 30$ V, varying V_1 . (b) Fixed $V_1 = 30$ V, varying V_2 .

varactor series connection reduces the overall capacitance to 0.49 pF–1.2 pF with the chip capacitor value $C_{dc} = 2.2$ pF. The C_{in} is selected as 0.6 pF as a tradeoff between tunability and loss, realized by an ATC 600S RF capacitor. The S -parameters of the filter were measured with an Agilent E5071C vector network analyzer.

The measured tunability of TZs and resonant frequencies are shown in Figure 8. Its corresponding resonant frequencies and TZs move toward high frequency when the reverse voltage applied on the varactor increases. Figure 8(a) shows that the TZ1 has a tuning range of about 440 MHz (1.96–2.40 GHz), while C_2 's bias voltage is fixed at 30 V. The TZ2 can be tuned from 1.40 GHz to 1.62 GHz as C_1 's bias voltage is fixed at 30 V, as shown in Figure 8(b). It is obvious that the low-side and high-side edges of the passband include TZs can be

Table 2. Comparison this work with others.

	T-MTT [12]	MWCL [10]	T-MTT [9]	This work
Elements (numbers)	Varactor (6)	Varactor (6)	Pin diode (2)	Varactor (4)
Biasing Voltage (V)	0–20	4–30	NA	0–30
In-band IL (dB) (Loss tangent)	1–3 (0.0027)	0.8 (min) (0.001)	1.35 (max) (0.0019)	0.4–1.1 (0.001)
3-dB FBW [tuning range (%)]	5.3–10 [4.7]	22–34 [12]	69.5–84.6 [15.1]	11.4–32.0 [20.6]
Separately tuned Tzs	✓	✓	×	✓
T_{zhigh} tuning range (%)	6.1	20.7	6.6	22.4
T_{zlow} tuning range (%)	6.9	14.6	20	13.6
Sideband rejection	10	13	9	10
Passband flatness among Tz tuning	×	✓	✓	×
Harmonic suppression	×	×	×	✓

adjusted independently, which increase the freedom on the bandwidth adjustment. Thus, both sides of the passband can be tuned by varying the capacitance of C_1 and C_2 .

The bandwidth tunable BPF measurement is presented in Figure 9, the -3 dB bandwidth ranges from 200 MHz to 560 MHz at a fixed center frequency, 1.75 GHz, with a insertion loss smaller than 1.1 dB. The simulated and measured results with harmonic suppression are shown in Figure 10. Obviously, they are in good agreement.

Table 2 compares the proposed filter with some recent state-of-the-art designs. It is summarized that the presented filter has the widest 3-dB FBW tuning range, quite low passband IL, minimum tuning elements, good harmonic suppression.

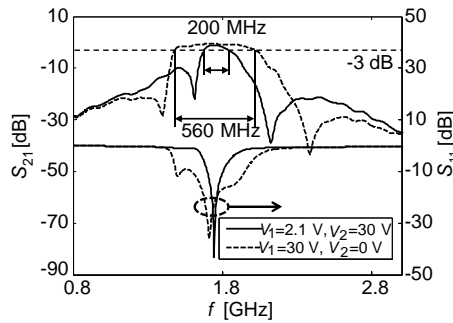


Figure 9. Measured S -parameters of the bandwidth tunable BPF.

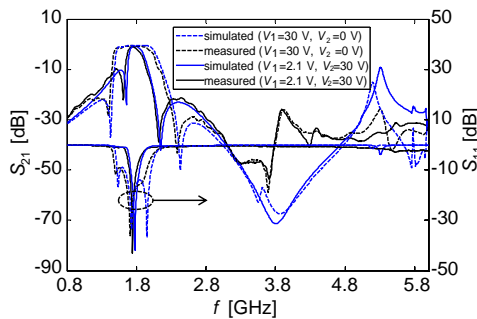


Figure 10. Measured S -parameters for the bandwidth tunable BPF with harmonic suppression.

4. CONCLUSION

In this paper, a bandwidth reconfigurable BPF with separate lower/upper sideband rejection and wideband harmonic suppression is demonstrated. With a constant odd mode and two independent varactor-tuned even modes and TZs, each passband edge can be adjusted freely. Compared with recent works, the proposed bandwidth tunable BPF has a -3 dB fractional bandwidth tuning range of 11.4–32.0%, a insertion loss of 0.4–1.1 dB and a wide out band suppression larger than 20 dB up to 6 GHz.

ACKNOWLEDGMENT

This work is supported by the National Natural Science Foundation of China under Grant 60990320, 60990323, 61271090 and the National 863 Propojt of China under Grant 2012AA012305.

REFERENCES

1. Chen, C. F., T. Y. Huang and R. B. Wu, "Design of dual- and triple-passband filters using alternately cascaded multiband resonators," *IEEE Transactions on Microwave Theory and Techniques*, Vol. 54, 3550–3558, 2006.
2. Tang, C. W. and P. H. Wu, "Design of a planar dual-band bandpass filter," *IEEE Microwave and Wireless Components Letters*, Vol. 21, 362–364, 2011.
3. Zhou, X. J., Y. J. Zhao, Y. Fu, and Y. Y. Liu, "Compact dual-mode tri-band microstrip BPF with three sets of resonators," *Progress In Electromagnetics Research Letters*, Vol. 33, 47–54, 2012.
4. Park, S.-J. and G. M. Rebeiz, "Low-loss two-pole tunable filters with three different predefined bandwidth characteristics," *IEEE Transactions on Microwave Theory and Techniques*, Vol. 56, 1137–1148, 2008.
5. Wang, X. G., X. H. Cho, and S. W. Yun, "A tunable combline bandpass filter loaded with series resonator," *IEEE Transactions on Microwave Theory and Techniques*, Vol. 60, 1569–1576, 2012.
6. Li, L. and D. Uttamchandani, "Demonstration of a tunable RF MEMS bandpass filter using silicon foundry process," *Journal of Electromagnetic Waves and Applications*, Vol. 23, Nos. 2–3, 405–413, 2009.
7. Xiang, Q. Y., Q. Y. Feng, and X. G. Huang, "Half-mode substrate integrated waveguide (HMSIW) filters and its application to tunable filters," *Journal of Electromagnetic Waves and Applications*, Vol. 25, Nos. 14–15, 2043–2053, 2011.
8. Tang, W. and J.-S. Hong, "Varactor-tuned dual-mode bandpass filters," *IEEE Transactions on Microwave Theory and Techniques*, Vol. 58, 2213–2219, 2010.
9. Kim, C. H. and K. Chang, "Ring resonator bandpass filter with switchable bandwidth using stepped-impedance stubs," *IEEE Transactions on Microwave Theory and Techniques*, Vol. 58, 3936–3944, 2010.
10. Huang, X., Q. Y. Feng, and Q. Y. Xiang, "Bandpass filter with tunable bandwidth using quadruple-mode stub-loaded resonator," *IEEE Microwave and Wireless Components Letters*, Vol. 23, 176–178, 2012.
11. Park, W.-Y. and S. Lim, "Bandwidth tunable and compact band-pass filter (BPF) using complementary split ring resonators (CSRRS) on substrate integrated waveguide (SIW)," *Journal of*

- Electromagnetic Waves and Applications*, Vol. 24, Nos. 17–18, 2407–2417, 2010.
12. Lacorte Caniato Serrano, A., F. Salette Corraera, T. P. Vuong, and P. Ferrari, “Synthesis methodology applied to a tunable patch filter with independent frequency and bandwidth control,” *IEEE Transactions on Microwave Theory and Techniques*, Vol. 60, 484–493, 2012.
 13. Park, S. J., K. Y. Lee, and G. M. Rebeiz, “Low-loss 5.15–5.70-GHz RF MEMS switchable filter for wireless LAN applications,” *IEEE Transactions on Microwave Theory and Techniques*, Vol. 54, 3931–3939, 2006.
 14. Chiou, Y.-C. and G. M. Rebeiz, “A quasi elliptic function 1.75–2.25 GHz 3-pole bandpass filter with bandwidth control,” *IEEE Transactions on Microwave Theory and Techniques*, Vol. 60, 244–249, 2012.
 15. Liu, B., F. Wei, H. Zhang, and X. Shi, “A tunable bandpass filter with switchable bandwidth,” *Journal of Electromagnetic Waves and Applications*, Vol. 25, Nos. 2–3, 223–232, 2011.
 16. Amir, T. and F. Keyvan, “Miniature harmonic-suppressed microstrip bandpass filter using a triple-mode stub-loaded resonator and spur lines,” *IEEE Microwave and Wireless Components Letters*, Vol. 21, 255–257, 2011.